IOPscience iopscience.iop.org

Home Search Collections Journals About Contact us My IOPscience

Photoluminescence and structure properties of $Zn_{1-x}Mg_xO$ films grown by RF magnetron sputtering

This article has been downloaded from IOPscience. Please scroll down to see the full text article.

2006 J. Phys.: Condens. Matter 18 1189

(http://iopscience.iop.org/0953-8984/18/4/007)

View the table of contents for this issue, or go to the journal homepage for more

Download details:
IP Address: 129.252.86.83
The article was downloaded on 28/05/2010 at 08:51

Please note that terms and conditions apply.

INSTITUTE OF PHYSICS PUBLISHING JOURNAL OF PHYSICS: CONDENSED MATTER

J. Phys.: Condens. Matter **18** (2006) 1189–1196 doi:10.1088/0953-8984/18/4/007

Photoluminescence and structure properties of $Zn_{1-x}Mg_xO$ films grown by RF magnetron sputtering

Xiao-Liang Xu[1], **Liu Lu, Ye Wang and Chao-Shu Shi**

Structure Research Laboratory, University of Science and Technology of China, Hefei 230026, People's Republic of China
and
Department of Physics, University of Science and Technology of China, Hefei 230026, People's Republic of China

E-mail: lism@ustc.edu.cn and xlxu@ustc.edu.cn

Received 30 June 2005, in final form 15 November 2005
Published 9 January 2006
Online at stacks.iop.org/JPhysCM/18/1189

Abstract

A number of $Zn_{1-x}Mg_xO$ ($x = 0$–0.16) films on Si(100) substrates were prepared by RF magnetron sputtering and annealed at different temperatures. X-ray diffraction (XRD) and atomic force microscopy (AFM) spectra indicate that the crystal structure of the films for $x > 0$ is the same as that of the hexagonal microcrystal ZnO. UV emission peaks for free excitons (and assisted phonon replicas) and electron–hole plasma (E–H) are found in the photoluminescence from the films, where the E–H has a superlinear five-times-enhanced lasing effect. The blue shift of the UV peaks in the photoluminescence spectra is found to be associated with increasing Mg content in the $Zn_{1-x}Mg_xO$ films, and the peak intensity is also reinforced significantly as the annealing temperature is increased. The green emission due to the oxygen vacancy was very weak, indicating that a good stoichiometry was maintained in the films. The minimum lasing threshold of the samples is 35 kW cm^{-2}, corresponding to ∼100 nm hexagonal microstructure.

(Some figures in this article are in colour only in the electronic version)

1. Introduction

Wide gap photoelectric materials and devices have played a very important role in increasing the light recording density and the light communications bandwidth. As a blue lasing material, GaN has attracted significant interest as a semiconductor light device [1]. Recent research on ZnO-based semiconductors has also revealed their potential applications in optical and electrical devices [2]. The study of the ZnO-based ternary compound was concentrated on

[1] Author to whom any correspondence should be addressed.

$Zn_{1-x}Mg_xO$ film and $ZnO/Zn_{1-x}Mg_xO$ multilayer or superlattice materials [2–11]. High quality $Zn_{1-x}Mg_xO$ layers have already been grown by many methods such as molecular beam epitaxy (MBE) [3–5], pulsed laser deposition (PLD) [6–8], metal–organic vapour phase epitaxy (MOCVD) [9], DC [10] or RF magnetron sputtering [11–13]. Among these, the magnetron sputtering method has several advantages: low cost, easier operation, low deposition temperature and obtaining p-type films by simply controlling the oxygen content in the growth [14]. Therefore, combining this with well-rounded silicon plane techniques, fabricating new silicon-based $ZnO/Zn_{1-x}Mg_xO/Si$ photoelectric devices using this method looks hopeful.

In this paper, attention is paid to the effect of annealing on the lasing properties of $Zn_{1-x}Mg_xO$ films grown by the RF magnetron sputtering method. The intention in this work is to fabricate $Mg_xZn_{1-x}O$ film with as low a lasing threshold as possible. Studies of low lasing threshold ZnO films can be found in the literature, where the records for the threshold were ∼30 kW cm^{-2} (grown by MBE) [15–17] and ∼40 kW cm^{-2} (grown by the VLS method) [18]. However, this appears to be the first time that low lasing threshold $Mg_xZn_{1-x}O$ films have been grown by RF magnetron sputtering. In this work, lasing thresholds as low as 35 kW cm^{-2} for samples fabricated with optimal growth and annealing conditions were obtained.

2. Experiment

The targets were prepared by a solid reaction method. A series proportion of 4N pure ZnO and MgO powders were mixed and ground in a carnelian mortar and pressed into a thin column bulk. The $Zn_{1-x}Mg_xO$ ceramic target was then prepared under 1200 °C for 5 h in air. The Mg contents x in the targets were 0, 8%, 12% and 16%. The targets were 60 mm in diameter.

$Zn_{1-x}Mg_xO$ films were grown in an RF magnetron sputtering system. The distance between the target and the Si(100) substrate was 70 mm, and the background vacuum of the system was 10^{-4} Pa. The sputtering power was 100 W and the discharge voltage 1000 V. 5N O_2 and 5N Ar were mixed to give the working gas. The O_2/Ar ratios were chosen as 1/3 following Cohen *et al* [10] and 1/1. The pressure was maintained as 3.0 Pa in the growth process. The deposition rate was 0.1 nm s^{-1}. The final thickness of the films was 300 nm.

Photoluminescence (PL) spectra, including PL excitation spectra (PLE, using Xe) and PL emission spectra (using a 325 nm Cd–He source, according to the PLE result), of the films were measured. The structure properties of the films were characterized by means of x-ray diffraction (XRD) spectra and atomic force microscopy (AFM).

3. Results and discussion

3.1. Photoluminescence

PLE spectra and PL emission spectra of the ZnO films grown under different conditions are shown in figure 1. The PLE was obtained by fixing the strongest emission peak at 380 nm and scanning the excitation wavelength; it indicates that the selected absorption wavelength of ZnO is 325 nm. The UV peak positions of the four samples are all around 3.34 eV, corresponding to emission from interstitial zinc (E_{ZnI}) which is 30 meV below the free exciton emission [19]. The second peak with energy at 3.20 eV should relate to two longitudinal optical phonon replicas (E–2LO). Actually the best ratio between the UV emission and yellow emission (due to oxygen vacancies in the material) is for the sample

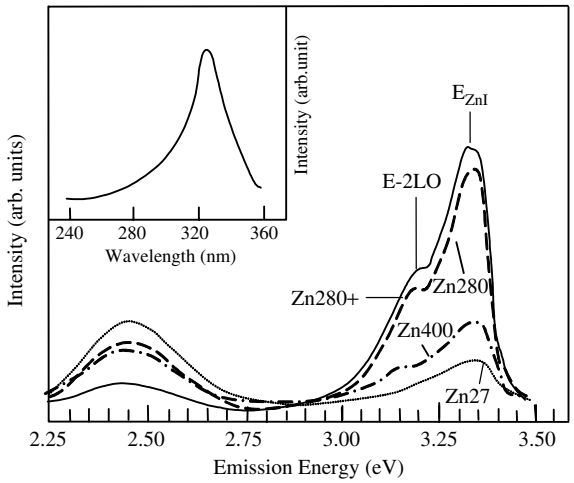

Figure 1. PL emission spectra of ZnO films grown under different conditions. The PLE spectrum is shown in the inset. Zn27, Zn400 and Zn280 are samples corresponding to the growth conditions $O_2/Ar = 1/3$ and $T_s = 27$, 400 and 280 °C, respectively. The sample Zn280+ was grown at $O_2/Ar = 1$ and $T_s = 280$ °C.

Zn280+. Therefore, the corresponding growth condition was chosen for the next $Zn_{1-x}Mg_xO$ film fabrication. It has been suggested by various authors that the substrate temperature (T_s) in the growth should be kept at RT [11], 300 °C [10] or 400–550 °C [12]. We used to suggest that $T_s = 150$ °C [20], on the basis of a photoluminescence study of samples grown at different temperatures. However, as the head of the temperature detector in a general RF magnetron sputtering system is usually fixed at the back of the sample holder, 150 °C is a vision temperature (T_v) which is different from the real T_s. $T_s = 1.9\ T_v$ was obtained in our growth system after calibration. Therefore the optimal T_s is 280 °C.

The $Zn_{1-x}Mg_xO$ films were grown on the same Si(100) substrate with different Mg contents: 8%, 12%, and 16%. The corresponding samples are called Mg8, Mg12 and Mg16, respectively. All the samples were annealed in air at 550 °C for one hour to remove the interstitial zinc [19]. The PL emission spectra excited by the 325 nm He–Cd laser were measured as shown in figure 2; a blue shift associated with increasing Mg content is shown by the free exciton emission (E_{ex}). The E–1LO ($E_{ex} - 75$ meV for Mg16 and -73 meV for Mg8, which are different from the -72 meV for pure ZnO) and E–2LO ($E_{ex} - 150$ meV for Mg16 and -146 meV for Mg8) are the energies for one and two longitudinal optical phonon assistance, respectively. At the lower energy shoulder of the UV peaks, there seems to be another structure, which may be due to electron–hole plasma (E–H) emission or emission from exciton–exciton collisions (P_n).

According to the formula [2]

$$P_n = E_{ex} - E_b^{ex}\left(1 - \frac{1}{n^2}\right) - \frac{3}{2}kT,$$

where $E_{ex} = 3.625$ eV (for Mg16) and $E_b^{ex} = 60$ meV are the free exciton energy and exciton binding energy, respectively, we then obtain that $P_2 = 3.541$ eV and $P_\infty = 3.526$ eV, which lie between E_{ex} (3.625 eV) and E2–LO (3.475 eV). Although E–1LO (3.550 eV) is close to P_2, changing the excitation intensity could help to distinguish them (see the analysis below).

To discern the relation between the crystallinity and optical properties of $Zn_{1-x}Mg_xO$ films, the annealing effect was studied. Four $Zn_{0.84}Mg_{0.16}O$/Si(100) samples were obtained

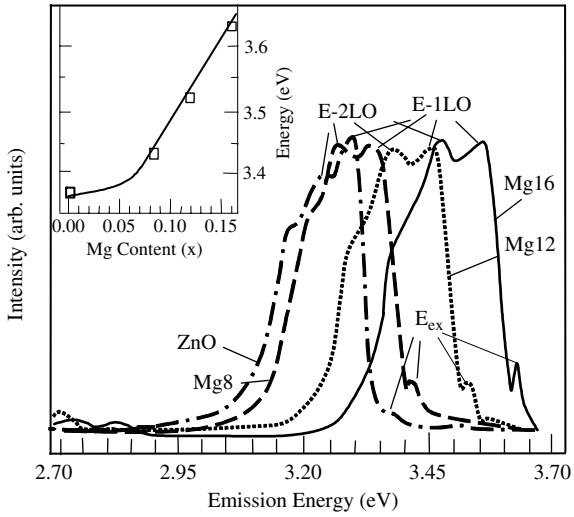

Figure 2. PL emission spectra of $Zn_{1-x}Mg_xO$ films with $x = 0, 8\%, 12\%$ and 16%. The excitation intensity is 50 kW cm^{-2}. The four squares in the small diagram correspond to the energy of free exciton emission (E_{ex}), shown by the simulating solid line from [21], due to the MBE growth data for $Zn_{1-x}Mg_xO$ alloy films obtained for band gap engineering.

by dividing up a big specimen grown under the same conditions as Zn280+. One of the samples was as grown and the other three were annealed at 400, 550 and 750 °C in air for 1 h.

The PL spectra excited by the 325 nm He–Cd laser were measured at room temperature, as shown in figure 3. In order to increase the excitation intensity (P), the laser facula was focused to 1 μm diameter. Therefore the highest excitation intensity is 170 kW cm^{-2}. Figure 3 indicates that the structure at the lower energy shoulder in figure 2 becomes more and more evidently with increasing annealing temperature. The structure may be mostly due to the E–H mechanism, which should have an energy red shift and a superlinear five-times-strengthening effect [15–17, 22]. The effect could be ascertained by measuring the integral intensity of the UV peak versus the excitation power. Since the He–Cd laser is not pulsed, the irradiated sample surface could be damaged by the strong laser beam—the nonlinear weakening effect gained prominence after $P \geqslant 50$ kW cm^{-2}, according to our data (see the inset in figure 3). Decreasing the sampling time can reduce the nonlinear effect. Comparing the slopes of the two simulated straight lines, when the excitation power intensity $P \leqslant 35$ kW cm^{-2}, the integral intensity of the emission is seen to be a fifth of that obtained for $P \geqslant 35$ kW cm^{-2}. On the other hand, an energy red shift from 3.44 eV (400 °C annealed) to 3.40 eV (750 °C annealed) is also found. Therefore, the simulated data had 35 kW cm^{-2} power density at the lasing threshold and a superlinear five-times-strengthening effect. For comparison, the 3.550 eV structure is linearly enhanced on increasing the excitation intensity; it is therefore related to E–1LO.

3.2. Structure

Figure 4 shows XRD patterns of $Zn_{0.84}Mg_{0.16}O$ films annealed at different temperatures. We observed the (002) main peak for all samples and (100), (101) and MgO(200) peaks only for the as-grown sample. These peaks (except the MgO(200) one) were indexed using the crystallographic data for the hexagonal structure of ZnO. At this composition ratio, the basic

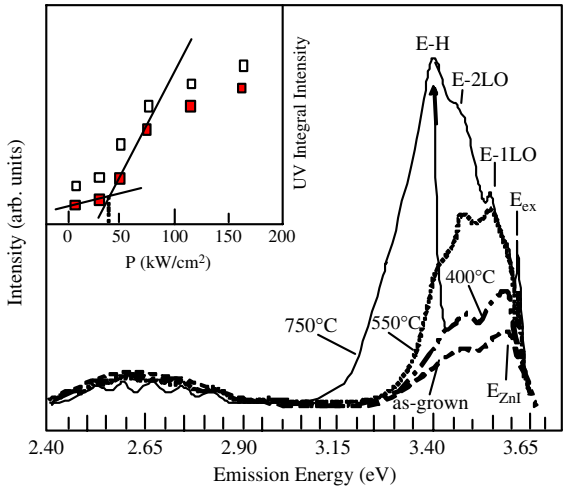

Figure 3. PL emission spectra for $Zn_{0.84}Mg_{0.16}O$ films annealed at 750, 550, 400 °C for 1 h and as grown, from top to bottom. The excitation intensity is 50 kW cm^{-2}. The red shift of the E–H peak is indicated by an arrow. The integral intensity of the UV peak from 750 °C/1 h annealed films as a function of the excitation intensity P is shown in the inset, where the sampling time for the solid square is the half that for the open square. Shortening the sampling time could decrease the irradiation damage of the film.

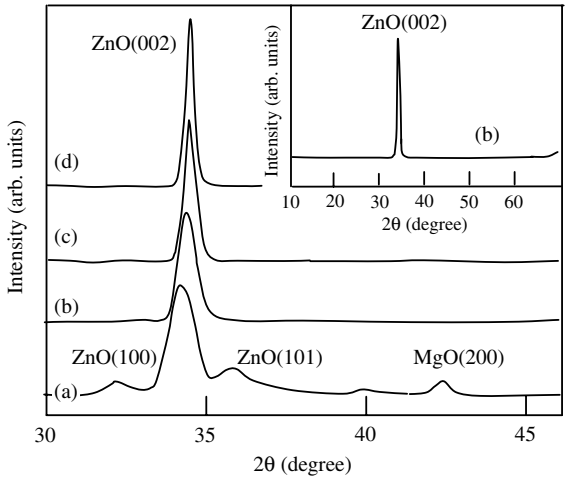

Figure 4. XRD patterns of $Zn_{0.84}Mg_{0.16}O$ films (a) as-grown and annealed at (b) 400 °C, (c) 550 °C and 750 °C in air for 1 h. The complete curve is shown for one temperature in an inset.

structure of $Zn_{1-x}Mg_xO$ is the same as that of ZnO, i.e. hexagonal. As the ion radii of Zn and Mg have nearly identical values, 0.74 and 0.71 Å, respectively [11], the strain caused by the replacement of each ion can be relaxed as the Mg content becomes smaller than 0.58 [11]. A ZnO(002) diffraction peak appears at about $34.4 \pm 0.2°$ in the scanning range of $2\theta = 10°$–$70°$ for all samples. This result indicates that the ZnO films are c axis oriented. Table 1 shows the FWHM and the positions of the XRD (002) peak and related rocking curve (001) peak.

As we increased the annealing temperature, the FWHM of the XRD (002) and the rocking curve (001) peak narrowed, and the peak positions shifted towards larger θ values; this may

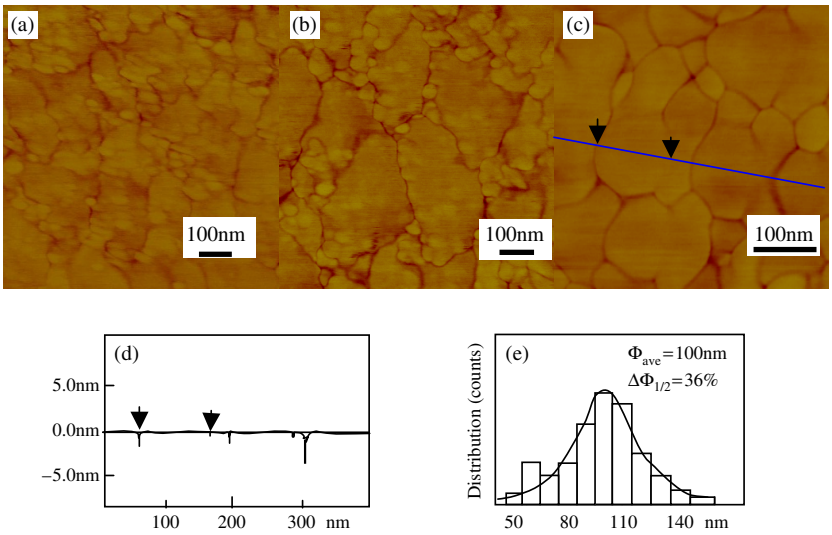

Figure 5. AFM image $Zn_{0.84}Mg_{0.16}O$ films (a) as-grown and annealed at (b) 550 °C, (c) 750 °C, plus (d) a lateral image of (c), and (e) the size distribution of the film annealed at 750 °C.

Table 1. FWHM and positions of the XRD (002) peak and the relative rocking curve (001) peak.

Sample number	Annealing temperature (°C)	(002) peak		(001) peak	
		Peak position (deg)	FWHM (deg)	Peak position (deg)	FWHM (deg)
No 1	As-grown	34.2	0.85	17.10	6.5
No 2	400	34.3	0.60	17.15	4.5
No 3	550	34.5	0.45	17.25	3.5
No 4	750	34.6	0.30	17.30	3.0

indicate a change of *c* axis [13] and improvement of the crystallinity. Annealing temperatures above 750 °C were not acceptable in our study, since a new ternary compound Zn_2SiO_4 should be produced at $T \geqslant 760$ °C [23, 24]. The change of the *c* axis can generally affect the band gap and some changes of the band gap will be reflected in some variation of the PL structure. However, we cannot find any obvious shift of the PL structures (except the E–H one) in figure 3. The answer can be found in the morphology analysis. The surface morphologies of the $Zn_{0.84}Mg_{0.16}O$ films annealed at different temperatures were studied by atomic force microscopy (AFM); see figure 5. Figure 5(a) is a surface photograph of the as-grown ZnO film, from which some shape accumulated from a number of 30 nm clusters can be seen. The XRD (002) peak of ZnO indicates the existence of ZnO microcrystal structure with some *c* axis orientation. The surface of the film becomes flatter upon annealing in air at 550 °C for 1 h, and a well-regulated grain boundary with hexagonal structure of the columns appears (see figure 5(b)). These columns have an obvious tendency to combine together into some bigger columns. Details of the growth kinetics of such columns can be found in the literature [15, 25]. These bigger columns get flatter and have a clear-cut hexagonal boundary with ∼100 nm side; also ⩽0.3 nm surface roughness was formed for the 750 °C annealed sample (see figures 5(c)–(e)). These changes of the morphology can therefore be included as two factors: (a) going from 30 nm clusters to 100 nm columns could significantly decrease the number of boundaries; (b) the improvement of the surface (and interface) roughness can shorten the gap between the

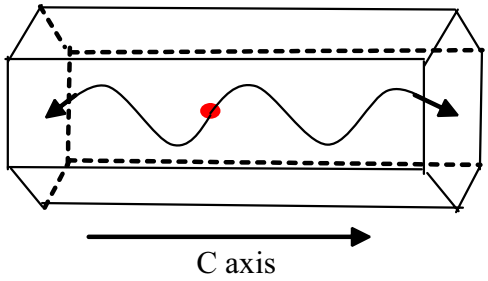

Figure 6. Schematic illustration of a nanocolumn as a resonance cavity with two naturally faceted hexagonal end faces acting as reflecting mirrors.

boundaries. These two factors are important reasons for the shift of the XRD (002) peak. As a matter of fact, such shifts of the (002) peak also appeared in some reported ZnO studies, in which there were also no position changes, except the E–H red shift, of the light emission structures [15–17, 20–24]. From the above analysis, the shortening of the *c* axis could be a subordinate factor in the shift of the (002) peak, which has no obvious effect on the band structure. On the other hand, when the scale of the clusters changes from 1 to 10 nm, the change in band gap can be reflected clearly by a shift of the light emission structure, namely a quantum scale effect.

Compared to other structures [15, 26], the hexagonal column structure can be easier to produce with a laser [15–18, 22–24]. As shown in figure 6, the pumped light is limited to the column and oscillates along the *c* axis between two end hexagonal planes, due to the power of the index at the edge of the column being greater than that of the index in the centre. Such columns therefore act as Fabry–Perot lasing cavities. Stimulated emission from the columns was collected in the direction along the nanowire's end plane normal (the symmetric axis) with a monochromator.

In conclusion, the study of $Zn_{1-x}Mg_xO$/Si layers used in the fabrication of low lasing threshold $Zn_{1-x}Mg_xO$ materials is important for the application of new silicon-based ZnO/$Zn_{1-x}Mg_xO$/Si photoelectric devices. Using the magnetron sputtering method combined with annealing, $Zn_{1-x}Mg_xO$ film on an Si(100) substrate with a lasing threshold as low as 35 kW cm^{-2} was successfully obtained in our study.

Acknowledgments

We thank Professor Hong-Tu Liu for valuable discussion. This work was supported by the National Natural Science Foundation of China under grant No 50472008 and Anhui Scientist Foundation under grants Nos 2003Z021 and 04022001.

References

[1] Nakamura S, Senoh M and Nagahama S 1996 *Appl. Phys. Lett.* **69** 4056
[2] Wang Z, Xu X and Chen Y 2004 *Acta Phys. Sin.* **53** 3924
[3] Harada C, Ko H-J, Makino H and Yao T 2003 *J. Cryst. Growth* **251** 623
[4] Ogata K, Koike K, Tanite T and Komuro T 2003 *Mater. Sci. Semicond. Proc.* **6** 539
[5] Ogata K, Koike K, Tanite T, Komuro T, Sasa S, Inoue M and Yano M 2004 *Sensors Actuators* B **100** 209
[6] Lorenz M, Kaidashev E M and von Wenckstern H 2003 *Solid-State Electron.* **47** 2205
[7] Choopun S, Vispute R D, Yang W, Sharma R P and Venkatesan T 2002 *Appl. Phys. Lett.* **80** 1529

[8] Sharma A K, Narayan J, Muth J F, Teng C W, Jin C, Kvit A, Kolbas R M and Holland O W 1999 *Appl. Phys. Lett.* **75** 3327
[9] Gruber Th, Kirchner C, Kling R and Reuss F 2004 *Appl. Phys. Lett.* **84** 5359
[10] Cohen D J, Ruthe K C and Barnett S A 2004 *J. Appl. Phys.* **96** 459
[11] Minemoto T, Negami T, Nishiwak S, Takakura H and Hamakawa Y 2000 *Thin Solid Films* **372** 173
[12] Lu J-G, Ye Z-Z and Chen H-H 2004 *Vac. Sci. Technol.* **23** 5 (in Chinese)
[13] Zhang X J, Ma H L, Ma J, Zong F J, Xiao H D and Ji F 2005 *Physica* B **357** 428
[14] Tuzemen S, Xiong G and Wilkinson J 2001 *Physica* B **308–310** 1197
[15] Xu X-L and Shi C-S 2000 *Prog. Phys.* **20** 356 (in Chinese)
[16] Ohtomo A, Kawasaki M and Sakuri Y 1998 *Mater. Sci. Eng.* B **54** 24
[17] Tang Z K, Yu P, Wong G K L and Kawasaki M 1997 *Nonlinear Opt.* **18** 355
[18] Huang M H, Mao S, Feick H, Yan H Q, Wu Y Y, Kind H, Weber E, Russo R and Yang P D 2001 *Science* **292** 1897
[19] Look D C, Hemsky J W and Sizelove J R 1999 *Phys. Rev. Lett.* **82** 2552
[20] Xu X-L, Wang L-Y, Wang Y, Yang Z-C and Shi C-S 2006 *Chin. Funct. Mater.* at press
[21] Matsumoto Y, Murakami M and Jin Z 1999 *Japan. J. Appl. Phys.* **38** L603
[22] Yu P, Tang Z K and Wong G K L 1998 *J. Cryst. Growth* **184/185** 601
[23] Xu X-L, Guo C-X and Qi Z-M 2002 *Chem. Phys. Lett.* **364** 57
[24] Xu X-L, Wang P and Qi Z-M 2003 *J. Phys.: Condens. Matter* **15** L607
[25] Maeda T, Yoshimoto M and Ohnishi T 1997 *J. Cryst. Growth* **17** 95
[26] Cao H, Wu J Y and One H C 1998 *Appl. Phys. Lett.* **73** 572